the figure is of a region close to the edge of the plate. The top boundary of the figure is subjected to a remote steady uniform tension. It is evident from Figure 2 that widespread continuum damage has taken place and the CDM calculations reported by Hayhurst et al [16] show that the damage formation is accompanied by considerable stress redistribution which, shortly after load up, produces an almost uniform stress across the minimum load bearing section of the plate. This leads to the result that the lifetime of the plate may be computed using the net section stress and uni-axial creep rupture data. The average experimental lifetimes are greater than the computed lifetimes by amounts equivalent to 3% and 7% on stress for the aluminium alloy and copper plates respectively. This result clearly shows the highly beneficial effects of stress redistribution, a similar plate was tested [22] in which the hole was replaced by a narrow slit of the same characteristic dimension. Again it was shown that stress redistribution rapidly nullified the initial high stress and strain gradients at the tip of the slit, and that the lifetime of the plate could again be predicted using the net section stress and uni-axial creep rupture data. The average experimental lifetimes are less than the computed lifetimes by amounts equivalent to 1% and 2% on stress respectively for the aluminium and copper plates containing slits. This result holds provided that the material behaves such that a major part of the strain is accumulated during tertiary creep [23].

4.2 Multi-Axial Stress Rupture Criteria

The creep rate Eq. (1) is given by:

$$\dot{\varepsilon}_{ij} = 3K\sigma_e^{n-1} s_{ij} t^m / 2(1-\omega)^n , \qquad (2)$$

where s_{ij} is the deviatoric stress = σ_{ij} - $\delta_{ij}\sigma_{kk}/3$, σ_e is the effective stress ($=(3s_{ij}\,s_{ij}/2)^{1/2}$), ω is the creep damage, and K, m and n are material constants.

The damage rate equation is given by:

$$d\omega / dt = M\Delta^{\chi}(\sigma_{ij}) t^m / (1+\phi)(1-\omega)^{\phi} , \qquad (3)$$

where $\Delta(\sigma_{ij})$ is the stress function $\alpha\sigma_1 + (1-\alpha)\sigma_e$, σ_1 is the maximum principal tension stress, and α, ϕ, and M are material constants. Eq. (3) can be normalised with respect to the uni-axial stress σ_o to yield normalised stresses $\Sigma_{ij} = \sigma_{ij}/\sigma_o$, $\omega = 0$ at $t = 0$, and $\omega = 1$ at failure to give:

$$\Delta(\Sigma_{ij}) = 1 = (\alpha\Sigma_1 + (1-\alpha)\Sigma_e), \qquad (4)$$

which defines the isochronous rupture surface in normalised stress space in terms of the parameter α [8].

In this section two materials will be discussed having different multi-axial stress rupture criteria. They are copper, for which α = 0.83 [18] which is approximately described by a maximum principal tension stress rupture criterion; and, an aluminium alloy for which α = 0, which is approximately described by an effective stress rupture criterion [8]. Both of these materials will be considered in this section when tested in an axi-symmetrically notched tension bar. The latter have been established as a practical laboratory technique for subjecting materials to high values of the first stress invariant J_1 (= σ_{ii}) and to low values of the effective stress σ_e.

A micrograph of a diametrical plane taken from a copper circular notched bar tested at 250°C until just before failure is shown in Figure 4. The figure shows a uniform state of damage which is synonymous with a relatively uniform state of stress and strain in the centre of the notch throat. This observation provides the justification for the use of the Bridgman testpiece [24] as a means of subjecting a relatively large volume of material to a relatively uniform state of complex stress.

Copper and aluminium notched bars when creep tested in this way show slight notch weakening and notch strengthening respectively. That is, for notch weakening the specimen has a rupture lifetime in excess of the lifetime of a plain bar tested at the net section stress. Copper shows typically 2% notch weakening and the aluminium alloy shows approximately 28% notch strengthening. As shown by Hayhurst et al [18] CDM is capable of predicting these results using Eqs. (2) and (3). The success of the approach is entirely dependent upon a knowledge of accurate values of the multi-axial stress rupture criterion α for both materials.

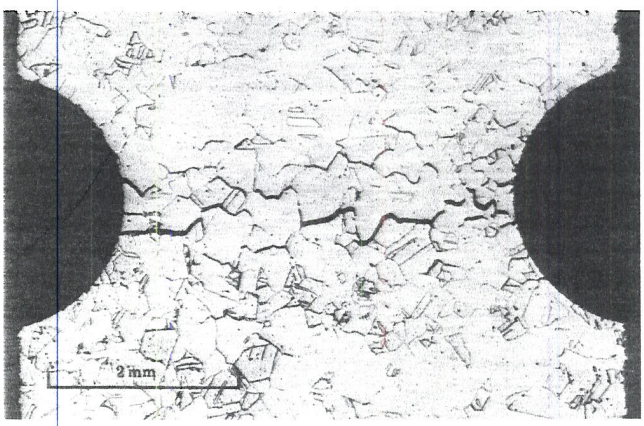

Figure 4. Micrograph of a diametral plane taken from an axi-symmetrically notched copper specimen tested at 250°C almost to failure under tension.

In design terms this is an important result, since in components which involve changes in section, and root radii, complex stress states are always generated. For these situations design calculation methods often assume that the rupture criterion is effective stress controlled (α = 0) when in fact many practical materials have α values approaching unity.

Hayhurst et al [18] have shown that when the circular notched bar geometry is replaced by the British Standard

V-notch geometry then damage accumulation behaviour becomes highly localised to the notch root. It is then more akin to damage evolution behaviour observed in creep crack growth. Despite this, CDM was shown [18] to be capable of predicting this localised behaviour and creep rupture lifetimes. This result gave the hint that CDM should be capable to predicting creep crack growth and led to a study of the behaviour of plane strain double-edged notched tension speciments [25], the results of which are outlined in the next section.

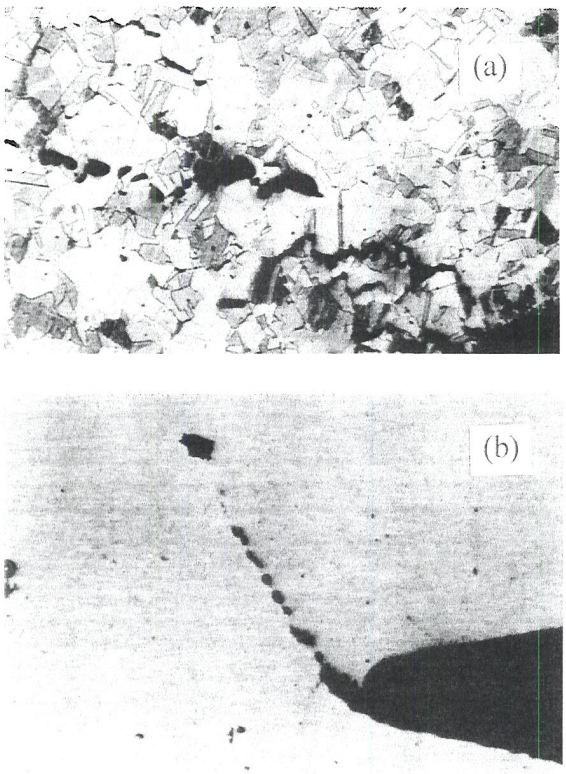

Figure 5. Mid-thickness micrographs of plane strain double-edge cracked tension specimens just before failure, (a) copper testpiece tested at 250°C and, (b) aluminium alloy testpiece tested at 210°C.

4.3 Prediction of Creep Crack Growth Using CDM

A double-edged cracked tension specimen was used to test creep rupture behaviour both in copper and in an aluminium alloy. The CDM prediction showed two dramatically different classes of behaviour. The copper testpiece showed a widespread redistribution of stress due to damage growth as shown in Figure 5a, the result being that the singularities in stress and strain at the cracked tip were quickly relaxed, and behaviour was quickly established close to that of net section stress control. Specimen lifetimes were very accurately predicted. In the case of the aluminium alloy testpiece the predicted behaviour closely agreed with that observed, which showed highly localised damage which had grown on a plane inclined at 67° to the notch plane as shown in Figure 5b. Damage growth by this mechanism took place at a decreasing rate until net section behaviour finally took over.

Both of these studies together with others on stainless steel double-edged cracked specimens, and on compact tension specimens [26] unambiguously demonstrated that CDM computations using the finite element solver DAMAGE XX [16, 18, 25] is capable of predicting creep crack growth from uni-axial creep data and a knowledge of the multi-axial stress rupture criterion of the material. For internally and externally cracked aluminium alloy and copper specimens, predicted and experimental lifetimes agreed to within an amount equivalent to 1% on stress. For the same specimens in Austenitic stainless steel experimental lifetimes are less than the computed values by an amount equivalent to 4% stress, and greater than the computed values by an amount equivalent to 2% on stress for internally and externally cracked specimens respectively. A further demonstration of the power of this approach is given in the next section by CDM computations carried out on superalloy notched bar testpieces having different ductilities.

4.4 Material Dependent Transition from Net Section Rupture to Creep Crack Growth

This has been demonstrated in a study on superalloy axi-symmetrically notched tension bar specimens. The geometry of the specimen is slightly different from that reported in section 4.2, the difference being that the depth of the notch is greater. The behaviour of two superalloys is described by the following constitutive equations:

$$\dot{\varepsilon}_{ij} = \frac{3As_{ij}\sinh\left(B\sigma_e\right)}{2\sigma_e\left(1-\omega_1\right)\left(1-\omega_2\right)^n}, \tag{5}$$

$$\dot{\omega}_1 = \frac{CA\left(1-\omega_1\right)\sinh\left(B\sigma_e\right)}{\left(1-\omega_2\right)^n}, \tag{6}$$

$$\dot{\omega}_2 = \frac{DA\left(\sigma_1/\sigma_e\right)^n N\left\{\sinh\left(B\sigma_e\right)\right\}}{\left(1-\omega_1\right)\left(1-\omega_2\right)^n}, \tag{7}$$

where $n = B\sigma_e \coth(B\sigma_e)$ and $N = 1$ for $\sigma_1/\sigma_e > 0$, and $N = 0$ for $\sigma_1/\sigma_e < 0$. The first damage state variable ω_1, models softening due to multiplication of dislocation sub-structures, and the second damage variable, ω_2, models softening due to grain boundary cavity nucleation and growth in nickel-based superalloys [12]. Following integration of these equations the failure ductility may be shown to be $\varepsilon_f = 1/3D$.

These equations may have been used with finite element computational CDM techniques for materials with two ductilities: (a) $D = 2$ ($\varepsilon_f = 15\%$), and $D = 128$ ($\varepsilon_f = 0.234\%$). The predicted damage distributions immediately before failure are shown in Figure 6. In both cases the

lifetimes are accurately predicted. For the high ductility material, Figure 6a, damage evolution has caused the stress to redistribute to a near uniform field in the notch throat. This has resulted in the evolution of a uniform damage field in the centre of the specimen, away from the notch throat, producing near classical widespread continuum behaviour. The opposite type of behaviour is shown in Figure 6b for the less ductile material where the initially high stresses at the root of the notch have not been able to redistribute sufficiently rapidly to avoid the formation of highly localised damage, and hence crack growth occurs. Stresses have re-distributed on a highly local scale ahead of the new crack tip which progressively moves inwards towards the centre of the specimen. The calculated stress distributions [27] show that peaks in the stress are maintained at any one instance ahead of the current crack tip.

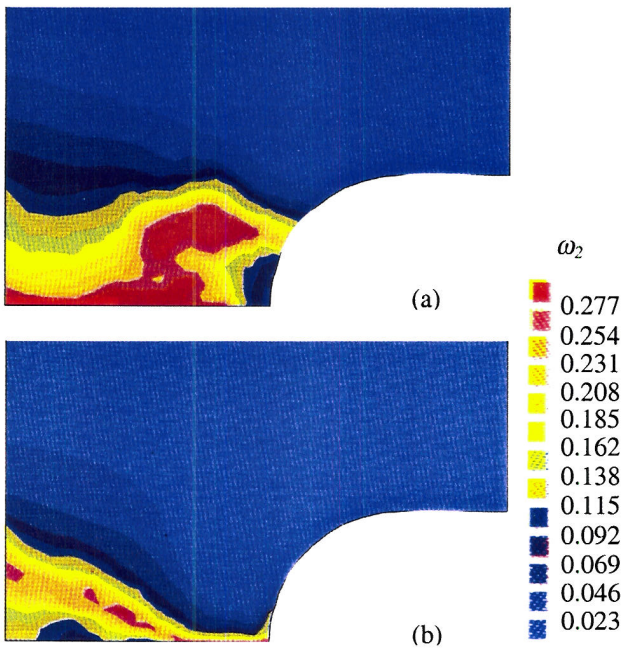

Figure 6. Damage variations, just before failure, over part of one quarter of a diametral plane of an axi-symmetrically notched bar. The left-hand and bottom boundaries denote axes of symmetry. Figure (a) is for high ductility material D=2 (ε_f=15%), and Figure (b) is for low ductility material D=128 (ε_f=0.234%).

The computations show unambigously that by reducing the material ductility from 15% to 0.234% the behaviour of the notched tension bar has been changed from widespread continuum rupture to the localised creep crack growth mechanism of failure. This result clearly demonstrates the requirement: that good creep ductility is mandatory for stresses to be beneficially redistributed in design applications. Failure to satisfy this requirement will result in structural failure at local stress raisers by creep crack growth.

4.5 Overview

It has been clearly demonstrated that finite element based computations made using CDM, with DAMAGE XX, are capable of predicting a wide range of behaviours from net-section stress dominated behaviour to creep crack growth from a knowledge of (a) uni-axial creep curves; (b) multi-axial stress tests; and (c) physically-based constitutive equations which incorporate (a) and (b). This has been shown to work exceedingly well provided that no mechanism changes take place. Should this occur then the models require recalibration from new test data. Operation over two or more mechanisms requires the assemblage of the complete set of equations within the Continuum Damage Mechanics calculations. The use or rejection of a particular set of equations is governed by the temperature, stress and stress state levels operating at a particular point within the structure as determined by the physics of the processes [10, 11].

Provided the mechanisms are modelled correctly then the approach forms a rational approach for remnant life predictions, which are so dependent on the extrapolation of short term data to the long term often encountered in component operation.

In the final section of the paper the prediction of the creep behaviour of multi-material structures is considered. The particular problem chosen is that of a branched ferritic steel welded steam pipe subjected to internal pressure at 590°C.

5. NON-LINEAR FRACTURE MECHANICS AND CDM PREDICTIONS OF CREEP CRACK GROWTH RATES IN A WELDED PRESSURISED PIPEWORK BRANCH CONNECTION

The purpose of this section is to compare the creep crack growth rate obtained using Continuum Damage Mechanics based model with the estimated rates obtained using the C^* method coupled with R5 code [5] for the weldment in an axi-symmetric equivalent of the Flank section of a pressurised pipework branch connection shown in Figure 7 [28].

5.1 Pressurised Pipework Branch Connection

The creep deformation and failure of a weldment in an axi-symmetric equivalent of the Flank section of a low alloy ferritic steel pressurised pipework branch connection has been analysed using the Finite Element CDM-based solver DAMAGE XX. A low alloy ferritic steel combination of 0.5Cr 0.5Mo 0.25V pipe-weld with 2.25Cr 1.0Mo weld metal (CMV weldments) has been used. The weld model is composed of four material